

Divertor power load feedback with nitrogen seeding in ASDEX Upgrade

A. Kallenbach, R. Dey, R. Dux, J.C. Fuchs, L. Giannone, A. Herrmann, H.W. Müller,
R. Neu, T. Pütterich, V. Rohde, W. Treutterer, ASDEX Upgrade Team
Max-Planck-Institut für Plasmaphysik, EURATOM Association, Garching, Germany

1 Introduction

Feedback control of the divertor power load is routinely used on ASDEX Upgrade to protect the divertor tungsten coatings [1]. The (thermo-) electric current into the outer divertor target is used as sensor signal [2], which is found to represent in good approximation the peak power load. To understand and further optimise the feedback system, an off-line model has been developed which includes a simple physics description for the plasma response.

2 Pre-processing for ELM removal

Divertor temperature and target power load are strongly modulated by ELMs. Radiative cooling controls the inter-ELM power load, other control tools are required for the ELM size and frequency. To obtain an undisturbed control of the inter-ELM heat load, ELMs have to be removed from the sensor signal, which is sampled at 100 kHz rate. This is realised by application of a modified median filter in the LabVIEW RT real time data acquisition, as shown in figure 1(left). The filter is adapted to the typical ELM frequency (50-300 Hz) and duration (0.5-3 ms) range in ASDEX Upgrade. It selects the 100st largest out of 700 values taken in the previous 7 ms, thus eliminating large ELM contributions but also negative spikes observed during the ELM start. The filter function is calculated each ms supplying ELM-cleaned signal to the discharge control system. The sensor data T_{div} represent in good approximation the inter-ELM peak power flux density, P_{max} , in the outer divertor, which is the quantity to be controlled for machine protection. Figure 1 shows a monotonic and approximately linear relationship of T_{div} and P_{max} . The two slightly different branches of T_{div} vs. P_{max} mainly represent high power discharges with N₂ seeding (improved confinement) and cold divertor plasmas caused by strong deuterium puffing. The latter show broader power load profiles, which can explain the higher T_{div} values for comparable maximum power flux densities.

3 Proportional-Integral (PI) controller for nitrogen puff rate

The nitrogen (N) puff rate is determined by means of a PI controller in the real time control system [3]. The core of the feedback algorithm is described by equation 1 for the N valve flux using the difference between set and actual divertor temperature, $T_{diff} = T_{set} - T_{div}$, where T_{div} is proportional to the median filtered target current.

$$\Phi_{valve} = \Phi_{ff} + K_p \cdot T_{diff} + \Phi_{integral} \quad (1)$$

The integral part is calculated for time point t as

$$\Phi_{integral} = \Phi_i^0 + K_i \cdot \int_{t_{start}}^t T_{diff} dt \quad (2)$$

K_p and K_i are the feedback gain coefficients for the proportional and integral parts. It is useful to divide the output flux of the feedback system into the fluxes resulting from the proportional and integral parts, as shown in figure 2. Here, also an additional small feedforward flux, Φ_{ff} , is seen, which had been introduced to optimise the feedback performance. Such a feedforward flux is no longer necessary after final optimisation of the gains.

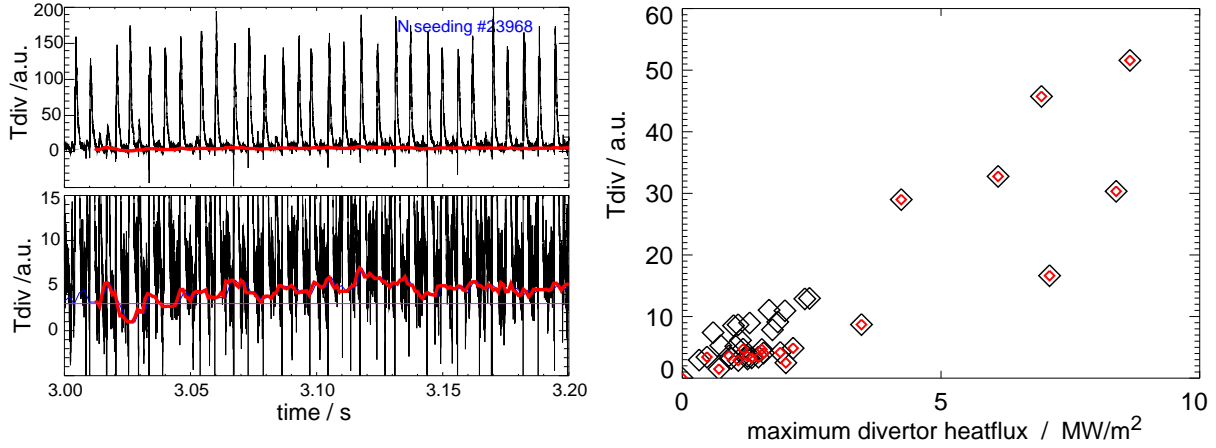


Figure 1: left: Thermoelectric current signal (black), multiplied by 0.02 to obtain approximate divertor temperature, and T_{div} obtained by median filtering. The off-line calculation (thick red line) was delayed by 6 ms to match the online signals (blue line), which are slightly delayed due to internal processing and transfer times. right: T_{div} vs. the inter-ELM peak power load in the outer divertor, obtained by median filtering of IR thermography data, for various H-mode discharges ($I_p=1$ MA, $B_t=-2.5$ T) with different heating powers and with and without nitrogen seeding. Data points marked with red diamonds have a confinement factor $H_{98y,2} > 0.9$.

For the initialisation of the controller, the start value of the integral part, Φ_i^0 , is important. Best results are obtained using $\Phi_i^0 = -K_p \cdot T_{diff}(tstart)$. This ensures that the gas flux remains at feedback switch-on, either zero or on its feedforward value. The gain coefficients largely determine the behaviour of the system. The proportional part K_p is responsible for quick reaction to transients, the integral part K_i determines how quickly and accurately the set value is reached. The ratio K_p/K_i is the time constant for the equilibrium approach of the system. A good first guess for the coefficients is obtained as follows: we assume a hot divertor transient with $T_{diff} = 10$ eV. A reasonable maximum N flux avoiding a H-L transition is $\Phi_{valve} = 1 \cdot 10^{22}$ el/s. From this, a first estimate leads to $K_p = -1 \cdot 10^{21}$ el/s/eV. The time constants for radiation build-up and pumping are about 50 and 100 ms, respectively, see section 4. Aiming at a slightly longer time constant K_p/K_i of about 0.2 s, the corresponding K_i is $-5 \cdot 10^{21}$ el/s/(s·eV). If other gases than N are used for radiative cooling, both K_p and K_i have to be scaled with the relative radiative capability of the seed gas compared to N. The radiative cooling rate $\Delta P_{rad}/n_Z$ scales roughly $\propto Z^3$ for core radiation [4]. Reasonable values for $K_{p,i}$ are obtained by scaling $\propto 1/Z^3$, resulting in about a factor 3 lower gains for Ne and a factor 17 lower gains for Ar in comparison to N. The gains should be optimised to achieve a fast and stable approach to the set value, to avoid large excursions of the flux and to produce an almost constant valve flux during quasi-stationary discharge phases. Higher gains result in quicker reactions, but have the danger of over-shooting or even oscillatory behaviour.

4 Simple plasma response model for PI gain optimisation

To allow off-line predictions of the feedback system behaviour and gain optimization, a model for the response of the divertor electric current on the seed gas flow is needed. The model is divided into three steps: first, the N content of plasma and divertor is calculated using the valve flow rate and the pumping speed. Second, the radiative power loss is determined using the N

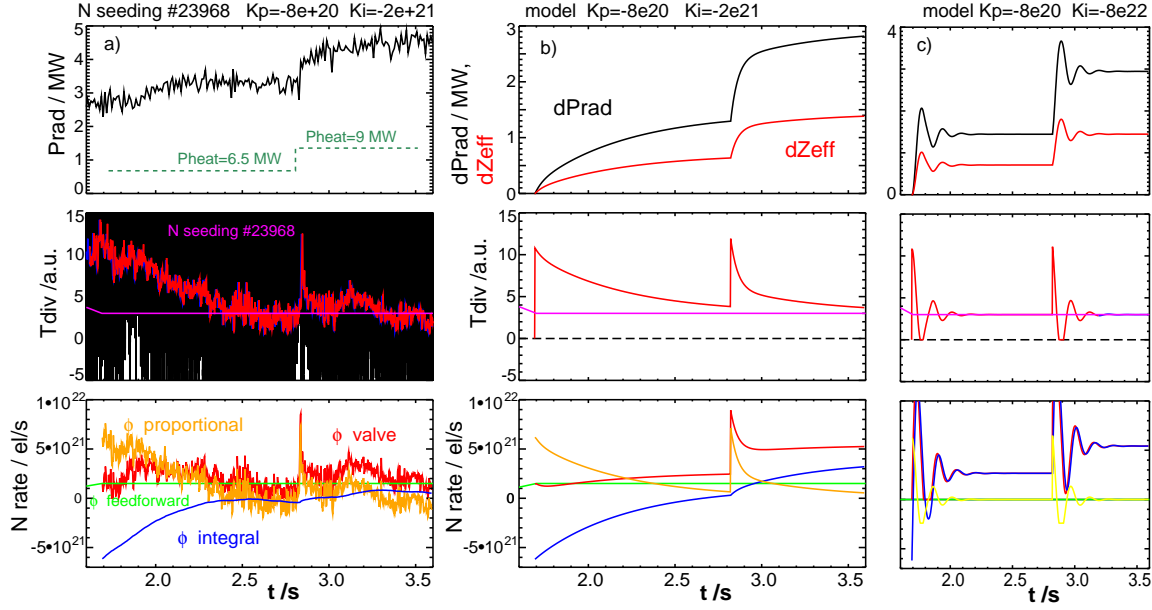


Figure 2: a) On- and offline calculated T_{div} , the N valve flux and the individual contributions of proportional and integral parts in the PI controller for # 23968. b) parameters obtained from the simple plasma response model. c) predicted behaviour for an assumed much larger value of K_i .

density and a simple radiation model. Finally, the divertor temperature and electric current are derived from an empirical scaling using the power flux entering the divertor. The response obtained by the plasma model is plotted in figure 2b for comparison with the measured behaviour.

The N content of main chamber and divertor is calculated using a simple particle balance model. A fixed distribution of the seed atoms between main chamber and divertor is assumed, which is described by a chamber model [5]. Parameters are the divertor N enrichment factor η_N , the main plasma and divertor volumes V_{main} and V_{div} , the pumping speed S_N and the experimental parameters average plasma density $n_{D,main}^i$ and divertor neutral deuterium density $n_{D,div}^0$. We assume ions to constitute the main chamber particle content and neutrals the divertor content. The N enrichment is then expressed as the ratio of N and D compression factors, $\eta_N = (n_{N,div}^0/n_{N,main}^i) / (n_{D,div}^0/n_{D,main}^i)$. Since the divertor neutral N content is not measured, estimates for η_N are used in combination with the measured main chamber ion densities and the neutral D divertor density to determine $n_{N,div}^0$. η_N can be determined experimentally from the decay rate of the N content after the injection phase [5]. Typical values used for ASDEX Upgrade are $V_{main} = 14 \text{ m}^3$, $V_{div} = 2 \text{ m}^3$, $S_N = 40 \text{ m}^3/\text{s}$, the discharges used for this paper have $\bar{n}_e = 8 \cdot 10^{19} \text{ m}^{-3}$ and $n_{D,div}^0 = 2.5 \cdot 10^{20} \text{ atoms/m}^3$. Assuming a stiff coupling of main chamber and divertor densities, effective volumes can be calculated to obtain the N densities in main chamber and divertor determining the radiative loss and the pumping rate. The particles remain in the effective volume

$$V_{eff} = V_{main} (1 + N_{N,div}/N_{N,main}) = V_{main} + V_{div} \eta_N n_{D,div}^0 / n_{D,main}^i \quad (3)$$

The time dependent N content of the main chamber plus divertor is then obtained by integrating

$$dN/dt = \Phi_{valve} - S_N N / V_{eff} \cdot (\eta_N n_{D,div}^0 / n_{D,main}^i) \quad (4)$$

where Φ_{valve} is the N valve flux in atoms/s. This simple model used to describe the particle recycling is valid as long as the pumping time is long compared to transfer times from SOL to divertor and divertor to SOL [6]. Under these conditions, the recycling pattern, and also the radiation distribution, is determined by the internal time constants and does not depend on the puff location. If the divertor enrichment gets large, or the pumping speed is very high, the simple 2-chamber approximation breaks down and divertor puffing can lead to higher divertor radiation in comparison to core puffing. The model neglects core particle transport (treated as infinitely fast) and profile effects, as well as wall pumping and storage which is observed with N seeding.

Having the impurity density in the main chamber and divertor specified, a simple scaling is used to calculate the additional radiative power loss caused by the seed impurity. In the following, approximate formulas for arbitrary seed species are given, defined by the atomic charge number Z . N stands for the total number of impurity atoms in the system. Similar to [7],

$$dP_{rad} = f_{rad} Z \bar{n}_e^2 A_{surf} dZ_{eff}, \quad dZ_{eff} = Z(Z-1)N/(V_{eff}\bar{n}_e). \quad (5)$$

A_{surf} is the plasma surface area, the assumed Z^1 dependence of the radiated power per Z_{eff} corresponds to a Z^3 dependence of the radiation with impurity density as introduced in section 3. The normalisation factor f_{rad} is calibrated against typical AUG H-mode discharges with medium gas puff and heating power, we obtain $f_{rad} = 1 \cdot 10^{-36} \text{ Wm}^4$. Finally, the divertor temperature and electric current have to be calculated using the divertor power flux. We use a modified version of an ELM averaged empirical scaling for AUG [2],

$$T_{div,scale} = f_{Tdiv}(\bar{n}_e/n_{Greenwald})^{-2} \times (P_{div} - P_{detach})/R_{geo} \quad (6)$$

where P_{div} is the power flux crossing the separatrix and P_{detach} the detachment power of the outer divertor where T_{div} becomes 0. $f_{Tdiv} = 4 \cdot 10^{-6} [\text{eV m} / \text{W}]$ is a normalisation constant derived from AUG measurements. The introduction of P/R in the scaling was motivated by its planned application to other devices like, e.g., ITER and the assumption that P/R is a divertor similarity parameter [8].

While the model described above is not expected to allow precise predictions of impurity levels etc., it contains all relevant elements for a realistic simulation of the radiative feedback. This allows to better understand and hence optimise the feedback system. E.g., inspection of figure 2 shows a fast reaction on the heating power step at $t=2.8$ s, but a relatively slow initial approach of the set value. Variation of the feedback parameters as well as plasma parameters suggests that a higher value of $K_i = -4e21$ can be used to achieve a quicker approach to the set value. A further increase of K_i leads to oscillatory behaviour as shown in figure 2c.

5 Conclusions

The radiative target power load control in ASDEX Upgrade, which became necessary after complete tungsten coating of the plasma facing components has been matured into a routine system, allowing high power discharges. A simple plasma response model has been developed which allows to optimise the system and to predict the performance in future devices.

References

- [1] A. Kallenbach et al., NF **49** (2009) 045007.
- [2] A. Kallenbach et al., JNM **290-293** (2001) 639.
- [3] W. Treutterer et al., Fus. Eng. Des. **81** (2006) 1927.
- [4] A. Kallenbach et al., Fus. Eng. Des. **36** (1997) 101.
- [5] A. Kallenbach et al., NF **35** (1995) 1231.
- [6] R. Dux et al., PPCF **38** (1996) 989.
- [7] G.F Matthews et al., JNM **241-243** (1997) 450.
- [8] K. Lackner, Comm. Pl. Phys. Contr. Fus. **15** (1994) 359.